Quantifying volcanic glass powder in cementitious systems using PONKCS-Rietveld analysis

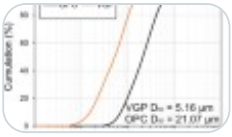

Original Article | Open access | 01 October 2025 | Article: 273

Innovative shear connections for cold-formed steel and concrete composite beams: experimental assessment by push-out tests

Original Article | 29 September 2025 | Article: 272

Experimental investigation on fatigue properties of asphalt mixtures with high content of RAP and recycled plastics

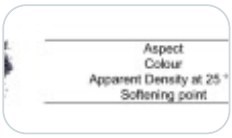

Original Article | Open access | 29 September 2025 | Article: 271

The impact of associated minerals in kaolinite clays on their physico-chemical characteristics for use as supplementary cementitious material

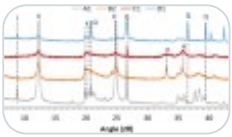

Original Article | 29 September 2025 | Article: 270

Bleeding of Portland composite cements

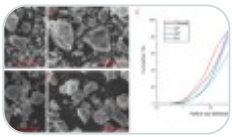

Original Article | Open access | 29 September 2025 | Article: 269

A molecular dynamics study on kaolinite-water-CMC mixture for 3D printing applications

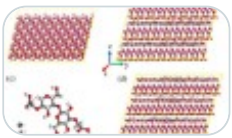

Original Article | 29 September 2025 | Article: 268

Designing 3D printable concrete by integrating the influence of aggregate characteristics

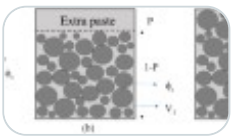

Original Article | 29 September 2025 | Article: 267

Durability assessment of MgO/hydromagnesite mortars—Resistance to chlorides and corrosion

Original Article | Open access | 20 September 2025 | Article: 266

Investigation of alkali-silica reaction in alkali activated cements by thermodynamic modelling

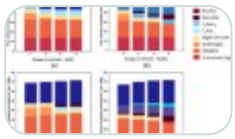

Original Article | Open access | 19 September 2025 | Article: 265

Comparison of field measured long-term prestressing force loss to design code equations for PSC girder

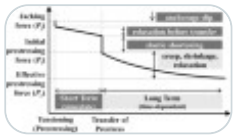

Original Article | 19 September 2025 | Article: 264

Assessment of moisture diffusion in hydraulic asphalt under coupled hydrothermal conditions

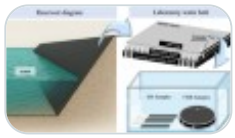

Original Article | 19 September 2025 | Article: 263

Field and laboratory characterization of the albedo of asphalt and horizontal surfaces

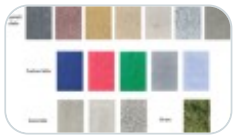

Original Article | Open access | 19 September 2025 | Article: 262

The influence of moisture content on the piezoresistive effect of CFRCM bundles during pull-out tests and the modification of its piezoresistive model

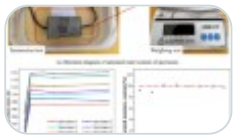

Original Article | 19 September 2025 | Article: 261

Hydro-chemo-mechanical constitutive modeling of cemented granular materials incorporating acid–base reactions

Original Article | 19 September 2025 | Article: 260

Experimental study of the fibre distribution in SFRC: a comparison between CT-scanning techniques and the inductive method

Original Article | Open access | 19 September 2025 | Article: 259

Integrated non-destructive assessment of 3D printed UHPC microstructure using X-ray computed tomography and ultrasonic waves

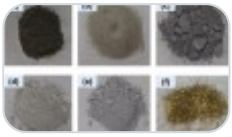

Original Article | 19 September 2025 | Article: 258

The effect of base bitumen properties on the performance of bitumen blends containing higher dosages of bio-ethanol industry-based lignin

Original Article | 19 September 2025 | Article: 257

The relationship between the paste properties and fine sand content in flowable concrete mixtures

Original Article | 19 September 2025 | Article: 256

Evaluating the reproducibility and consistency of different sample preparation techniques used for ATR-FTIR spectroscopy from the RILEM 295-FBB TG1 round robin test

RILEM TC Report | Open access | 19 September 2025 | Article: 255

Stochastic analysis of 3D concrete printing process with curvature and inclination by explainable data-driven modelling

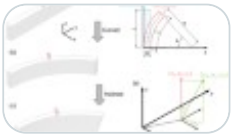

Original Article | 19 September 2025 | Article: 254

Assessing structural integrity of fly ash-based geopolymers with different modifiers under microbial-induced corrosion in real-world environments

Original Article | 19 September 2025 | Article: 253

Carbonation-induced corrosion of steel in sodium carbonate alkali-activated slag

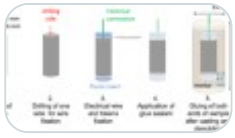

Original Article | Open access | 18 September 2025 | Article: 252